JOURNAL OF MATERIALS SCIENCE **37** (2002) 2351 – 2358

Thermal and morphological characterization of poly(ethylene terephthalate)/calcium carbonate nanocomposites

M. L. DI LORENZO*, M. E. ERRICO, M. AVELLA
Istituto di Ricerca e Tecnologia delle Materie Plastiche (C.N.R.) - c/o Comprensorio Olivetti, Fabbr. 70 - Via Campi Flegrei 34, 80078 Pozzuoli (NA), Italy
E-mail: diloren@irtemp.na.cnr.it

Nanocomposites composed of poly(ethylene terephthalate) (PET) filled with calcium carbonate particles of nanometer scale were prepared by polymerizing the polyester in the presence of the nanosized fillers. Besides plain calcium carbonate, carbonate nanoparticles coated with stearic acid were also used, in order to improve the compatibility between the polymeric matrix and nanofillers. Morphological analysis evidenced a good dispersion of both the nanopowders into the PET matrix, especially in the case of coated calcium carbonate. The strong interfacial adhesion between the two phases is also responsible for the increase of the glass transition and melting temperatures in the nanocomposites compared to plain PET. Finally, non-isothermal crystallization studies revealed that the coated $CaCO_3$ is a good nucleating agent for PET. Analysis of non-isothermal crystallization data with the Ozawa theory was successful for plain PET and PET/un-$CaCO_3$, but this method failed to describe the dynamic solidification of the PET/c-$CaCO_3$ nanocomposite.
© *2002 Kluwer Academic Publishers*

1. Introduction

Polymer composites are widely used in areas of electronics, transportation, construction and consumer products, as they offer unusual combinations of properties that are difficult to obtain from individual components. Fillers are generally in the form of fibers or platelets. The nature of the fillers, including their composition, dimensions, homogeneity of dispersion and adhesion level in a polymeric matrix, is important for the bulk properties of the composites. In the last years nanoparticles have become of interest as fillers for polymeric matrices. Nanocomposites are defined by the particle size of the dispersed phase having at least one dimension of less than 10^2 nm [1]. Because of the nanoscale dimensions, nanocomposites possess superior physical and mechanical properties compared to the more conventional microcomposites, and therefore offer new technology opportunities.

Three types of nanocomposites can be distinguished, depending on the number of dimensions of the dispersed particles that are in the nanometer range. When the fillers are nanosized in the three dimensions, they are practically isodimensional, such as spherical silica nanoparticles obtained by *in situ* sol-gel methods [2] or by polymerization promoted directly from their surface [3]. When two dimensions of the fillers are in the nanometer scale and the third is larger, forming an elongated structure, the reinforcing particles are generally named nanotubes or whiskers, such as carbon nanotubes [4] or cellulose whiskers [5, 6]. Finally, nanocomposites of the third type contain reinforcing particles that have only one lateral dimension in the nanometer range: the fillers have the shape of sheets that are a few nanometers thick with a length of the order of microns [7].

The present work deals with nanocomposites of the first type, composed of calcium carbonate ($CaCO_3$) nanoparticles dispersed in a thermoplastic matrix [poly(ethylene terephthalate) (PET)]. Two types of nanoparticles were used: one type was made of plain $CaCO_3$, the other kind was composed of $CaCO_3$ coated by stearic acid, an inorganic coating. 2% of each filler was added to the polyester matrix. The aim is to analyze the effect of the type of the reinforcing agent on the properties of PET, and in particular to determine the efficiency of the stearic acid coating in improving dispersion into the polyester matrix and promoting interfacial adhesion between the phases. The composites were prepared by polymerizing PET in the presence of the reinforcing particles. Direct blending of the polymeric matrix with the filler by melt mixing has received only a limited number of successful results, due to the high tendency of the nanosized fillers to form larger clusters during blending, that limits the advantages of their small dimensions [7, 8]. Conversely, the *in situ* preparation methodology has

*Author to whom all correspondence should be addressed.

been proven to provide nanocomposites with enhanced properties [9, 10].

The results concerning the influence of $CaCO_3$ nanoparticles on the structure and crystallization process of poly(ethylene terephthalate) (PET) are reported in this paper. In particular, the effect of the addition of nanoparticles on non-isothermal solidification of PET is investigated. Analysis of non-isothermal crystallization kinetics of polymers is of enormous importance, since the crystalline structure and morphology, and thus the properties of a material, strongly depend on the conditions under which a polymer solidifies from the melt, especially in the presence of foreign substances that can act as potential heterogeneous nuclei. Therefore, in order to reach the optimum conditions for industrial processes and to obtain products with tailored properties, it is necessary to have quantitative evaluations of non-isothermal crystallization rates [11].

2. Experimental part

2.1. Materials

Dimethylterephthalate (DMT), Aldrich reagent-grade product, ethylene glycol (EG), Aldrich spectrophotometric-grade product, and zinc acetate, BDH reagent-grade product, were used without further purification.

Calcium carbonate nanoparticles, plain and coated with stearic acid, were kindly supplied by Solvay & Cie. Literature data indicate that the nanoparticles do not undergo degradation phenomena at the temperatures used for polymerization of PET [12].

2.2. Preparation of PET and PET/ceramic nanocomposites

Plain PET was synthesized following a standard procedure reported in the literature [13]. This method was properly modified to allow insertion of the nanoparticles during polymerization.

In a cylindrical reactor suited with side arms for refrigeration, distillation and mechanical stirring, 272 g of dimethylterephthalate, 200 g of ethylene glycol and 0.22 g of zinc acetate were added. Before the reaction, all traces of water were removed from the reactor. The reagents were melted by submerging the reactor halfway in a heating oil bath at 197°C. The reaction was carried under a continuous nitrogen flux and vigorous stirring. Methyl alcohol distilled rapidly in a few minutes. After 1 hour the reactor was adjusted to be heated as completely as possible and was kept at 197°C for 2 hours more. The reactor was then heated at 222°C for 15 min, in order to distil excess glycol and remove all traces of residual methanol. Then the reactor was heated at 283°C and 2% by weight of calcium carbonate nanoparticles, calculated with respect to the amount of DMT, were added. As polymerization started, glycol distilled. After $5 \div 10$ min vacuum was applied very cautiously and the pressure brought to less than 0.2 torr. Polymerization was complete within 3 hr. The reactor was then filled with nitrogen, removed from oil bath and allowed to cool.

Throughout the article, the nanocomposites containing uncoated calcium carbonate (un-$CaCO_3$), and calcium carbonate coated with stearic acid (c-$CaCO_3$) are identified as PET/un-$CaCO_3$ and PET/c-$CaCO_3$ respectively.

2.3. Preparation of compression-molded sheets

Plain PET and PET nanocomposites were compression-molded in a heated press at 300°C for 5 min without any applied pressure. After this period, a pressure of 100 bar was applied for 5 min, then the press platelets, containing coils for fluids, were rapidly cooled to room temperature by cold water. Finally, the pressure was released and the mold removed from the plates. Films of 0.15 mm thickness were produced.

2.4. Scanning electron microscopy

Morphological analysis of the compression-molded samples was conducted with a SEM Philips XL 20 series microscope. Small pieces of the compression molded samples were kept in liquid nitrogen for 5 minutes and fractured. Before the electron microscopy observation, the surfaces were coated with Au-Pd alloy with a SEM coating device (SEM Coating Unit E5150 - Polaron Equipment Ltd.).

2.5. Calorimetric measurements

The thermal properties were measured with a differential scanning calorimeter Mettler DSC-30. The apparatus was calibrated with pure indium, lead and zinc standards at various scanning rates.

Non-isothermal crystallizations were performed using the following temperature program. Each sample was heated from 0 to 300°C at a scanning rate of 20°C/min, kept at this temperature for 10 min to allow complete melting, cooled to room temperature at five different scanning rates: 0.5, 1, 2.5, 5 and 10°C/min, then heated at 20°C/min. Dry nitrogen gas with a flow rate of 20 ml min^{-1} was purged through the cell. For each sample the glass transition temperatures (T_g) were taken as the temperatures corresponding to the maxima of the peaks obtained by the first order derivative traces of the DSC thermoanalytical curves. The melting temperatures (T_m) were measured as the maxima of the endothermic peaks of the DSC curves. The crystalline fractions (X_c) were calculated by integration of the melting endotherms, using the literature data for the enthalpy of fusion of PET in the fully crystalline state of 140 J/g [14].

2.6. Thermogravimetrical analysis

The thermal stability of the samples was measured by means of thermogravimetrical analysis (TG) with a TC 10A Mettler TG equipped with a M3 analytical thermobalance, by recording the weight loss as a function of temperature. Each sample was heated from 40 to 700°C at a scanning rate of 20°C/min in air atmosphere. The degradation temperature (T_d) was taken as the temperature corresponding to the maximum of the peak obtained by the first order derivative trace.

3. Results and discussion

In order to determine the morphology of the nanosized powder samples, the $CaCO_3$ nanoparticles were observed as obtained by means of scanning electron microscopy (SEM). The electron micrographs of the two types of fillers are presented in Fig. 1. For both the samples the nanoparticles have a strong tendency to form aggregates whose dimensions are much higher than those of the isolated particles. Both the types of $CaCO_3$ particles have a spherical appearance. The average diameter of the un-$CaCO_3$ particles is about 40–50 nm, whereas the c-$CaCO_3$ particles are slightly larger, with dimensions of about 60–80 nm. It must be taken into account that, in order to make the samples visible under the scanning electron microscope, the nanoparticles were coated with 18 nm of Au-Pd alloy. With thinner coverings it was impossible to obtain a clear SEM image. Since the covering is of the same order of magnitude of the particles size, it is likely that the real dimensions of the samples are smaller than the measured ones.

PET based nanocomposites were prepared by means of "*in situ* polymerization" methodology, dispersing the calcium carbonate nanoparticles within the matrix

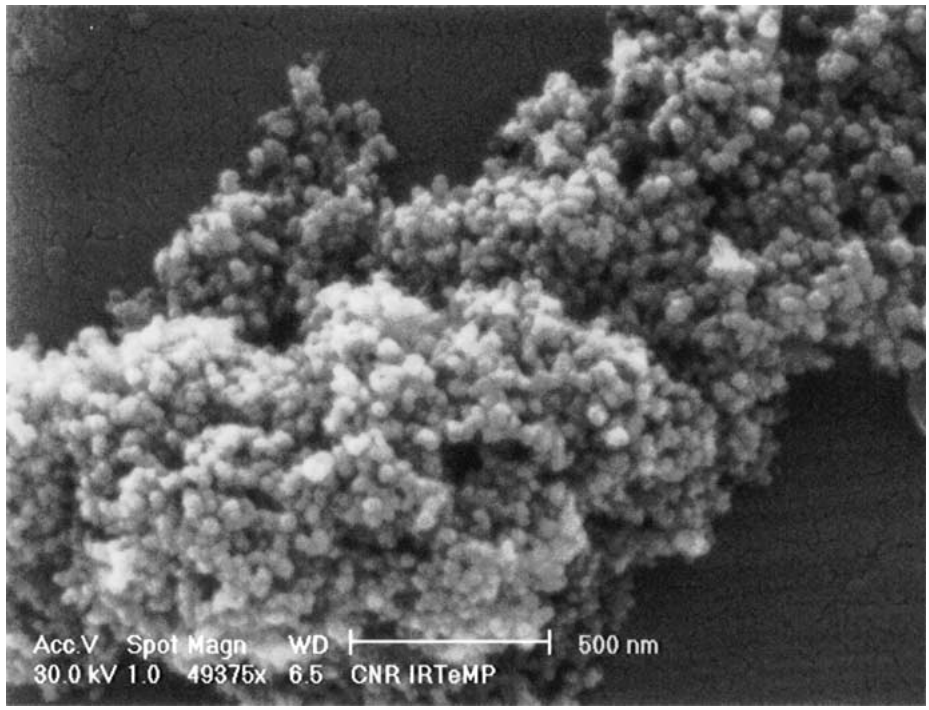

(a)

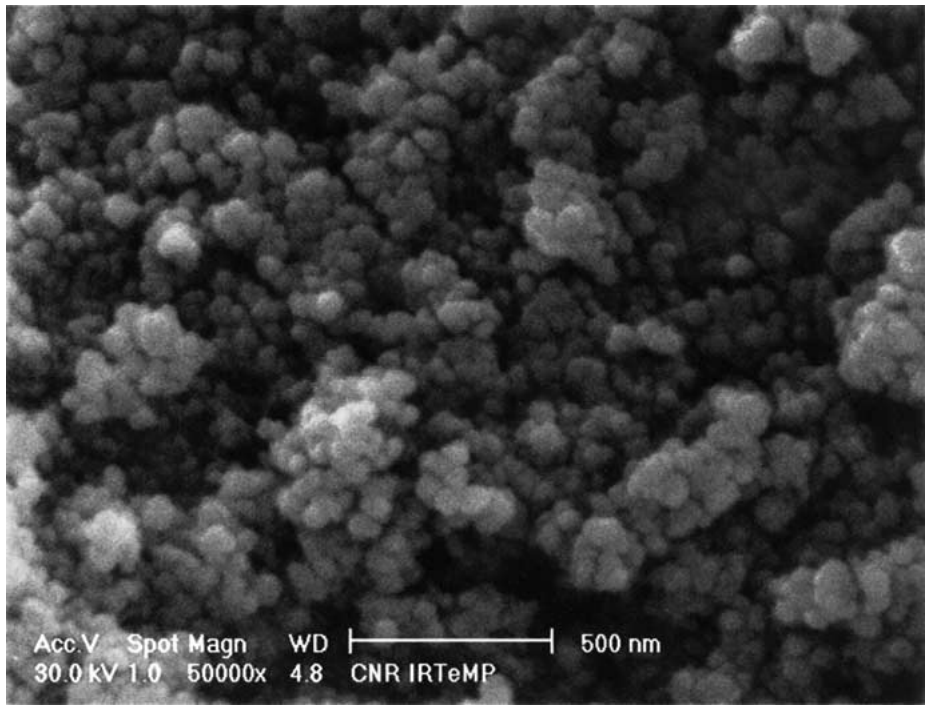

(b)

Figure 1 Scanning electron micrographs of the ceramic nanoparticles: (a) un-$CaCO_3$; (b) c-$CaCO_3$.

during polymerization of the polyester. This preparation method was selected in order to obtain a large matrix/nanofiller interface and a homogeneous dispersion of the $CaCO_3$ nanopowders in the PET matrix [9, 10]. PET was synthesized by polycondensation reactions, following a conventional procedure reported in the literature [13]. The nanofillers were introduced in the reactor only when the reaction that leads to production of the polymeric precursor, ethylenterephthalate (ET) had reached completion. This way, a possible interaction of the ceramic nanoparticles with DMT and EG reagents, that may result in incomplete ET production, is avoided. The polycondensation reaction starts in the liquid phase, containing ET and the nanofillers, and the viscosity of the solution increases with the conversion grade of the monomer, which raises the molecular mass of PET. In this way a fine dispersion of the nanopowders in the reaction mixture can be obtained, due to the vigorous mechanical stirring, and to the possibility that the nanoparticles might be captured by the growing polymer chains with the increase of mixture viscosity [9, 10].

In Fig. 2 the scanning electron micrographs of the nanocomposites are exhibited. In the sample reinforced

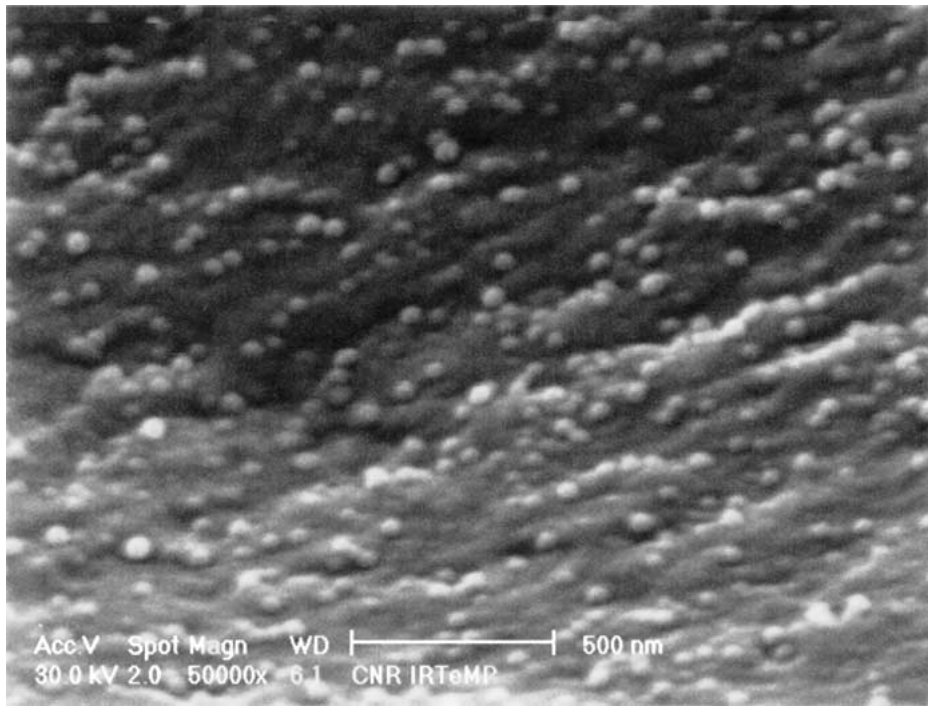

(a)

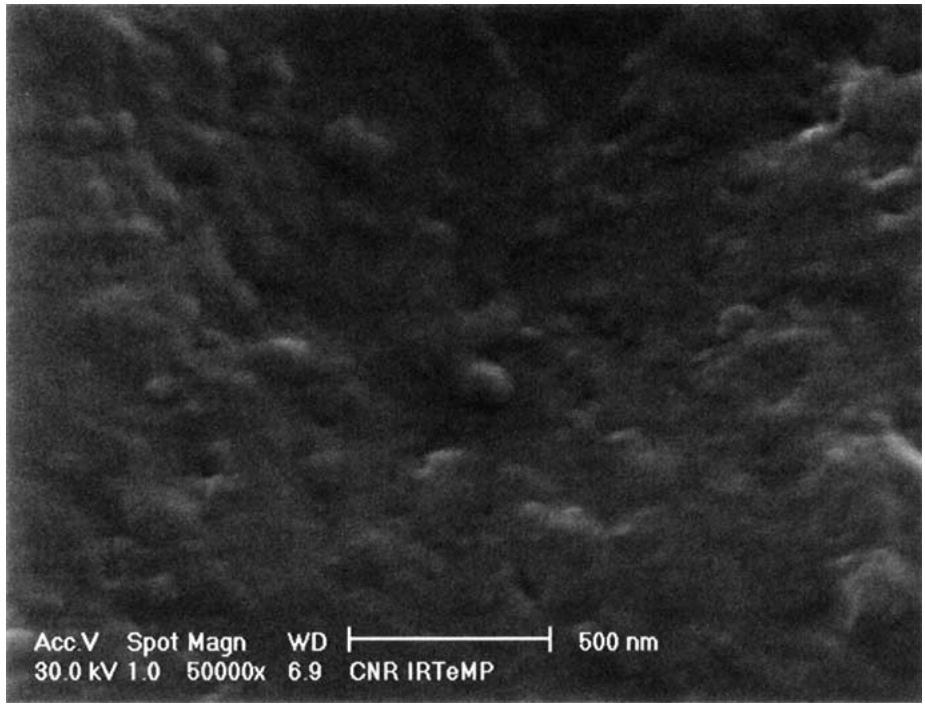

(b)

Figure 2 Scanning electron micrographs of the PET/ceramic nanocomposites: (a) PET/un-$CaCO_3$; (b) PET/c-$CaCO_3$.

TABLE I Thermal parameters of PET and PET nanocomposites: Decomposition temperature (T_d), glass transition temperature (T_g), melting temperature (T_m) and crystallinity (X_c)

Sample	T_d (°C)	T_g (°C)	T_m (°C)	X_c (%)
PET	486	69	251	35
PET/un-$CaCO_3$	498	74	249	31
PET/c-$CaCO_3$	500	83	259	37

with un-$CaCO_3$ (Fig. 2a) a high number of very small discrete particles, quite welded to the matrix, is observable. In the PET/c-$CaCO_3$ sample (Fig. 2b) the discrete particles are still evident, but they are larger and better welded to the PET matrix, suggesting that the coating of $CaCO_3$ with stearic acid can promote adhesion between the nanosized reinforcement and the polyester matrix. The improved compatibility between the phases is probably due to the hydrophobic characteristics of the c-$CaCO_3$ sample imparted by the stearic acid coating, as reported in the literature for similar nanocomposite systems [15–19].

The morphological analysis revealed that addition of the $CaCO_3$ nanofillers during the synthesis of PET can provide a useful method of preparation of the nanocomposites, with the achievement of good dispersion and adhesion levels.

The thermal stability of PET and PET nanocomposites was analyzed with thermogravimetry. The values of the degradation temperature (T_d), that correspond to the maximum of weight loss rate, are presented in the second column of Table I. The presence of nanoparticles raises the degradation temperature of the material of about 15°C. Thermal degradation of PET is initiated by random scission of the chains at the ester linkages, leading to carboxyl and vinyl ester end groups [20]. The primary degradation products undergo secondary processes (decarboxylation, hydrogen transfer, transesterification) to give a wide variety of substances, like carbon oxides, aldehydes, hydrocarbons, as well as aromatic acids and their esters. These reactions are additionally complicated by the presence of oxygen that actively participates in the process. It has been suggested that in the presence of oxygen, thermal degradation starts by formation of hydroperoxides at the methylene groups, followed by homolytic chain scissions [21]. However, the overall mechanism is rather complex and still needs a reasonable explanation [22]. The $CaCO_3$ particles, finely dispersed within the PET matrix, probably interfere with the degradation mechanism, slightly retarding it.

The glass transition temperatures (T_g) of the samples were measured by DSC after melting the samples at 300°C for 10 min and cooling at 10°C/min. The relative thermoanalytical plots are shown in Fig. 3. From the curves the glass transition temperatures were measured, and their values are reported in the third column of Table I. The T_g of plain PET is about 69°C, in agreement with literature data [14], whereas higher values were observed for the two reinforced samples. In particular, the presence of c-$CaCO_3$, that can better adhere to the polyester matrix, raises the T_g of PET of 14°C. The presence of a rigid filler into a polymer matrix is

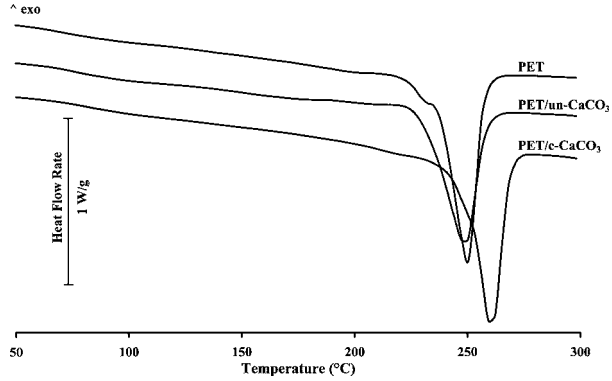

Figure 3 DSC thermoanalytical curves of PET and PET ceramic nanocomposites measured on heating at 20°C/min, after cooling from the melt at 10°C/min.

generally responsible of a slight increase of the glass transition temperature, usually of about 4–6°C, respect to the neat polymeric matrix [23]. In the present case of PET/$CaCO_3$ nanocomposites, the increase is larger than in the more conventional micro-composites. This result is justified by the homogeneity of dispersion of the nanofillers into PET, as revealed by SEM analysis, and by the enormous interfacial area of the nanoparticles, as the strong interconnection between the two phases reduces the mobility of PET chains [9]. This is particularly evident for PET/c-$CaCO_3$ nanocomposite, where the presence of the organic coating on the nanoparticles surface produces a better matrix/filler interfacial adhesion.

The crystallization kinetics studies of PET and the nanocomposites were conducted in dynamic conditions by cooling the samples from the melt at various scanning rates. The analysis of polymer crystallization in non-isothermal conditions must be performed with care, as it can be complicated by the possible occurrence of thermal gradients within the sample and between the cooling furnace and the sample [11, 24–26]. In addition, crystallization is an exothermic process and the heat developed during the phase transition may cause some local heating and create additional thermal gradients within the sample. As a consequence, transitions can occur at temperatures that do not correspond to those detected by the instrumentation. The thicker the sample, the more critical this problem is. In order to limit the problems due to thermal lags, for the present analysis the scanning rate was limited to 10°C/min, and 0.15 mm thick samples, of approximately 3 mg, were used.

The results obtained studying the non-isothermal solidification process of PET nanocomposites showed that the mechanism of phase change depends on cooling rate and composition. For every sample, with increasing the cooling rate, χ, the crystallization curves shift to lower temperatures, as shown in Fig. 4 for the sample reinforced with 2% un-$CaCO_3$. The same trend was observed for the other two samples. At lower χ there is more time to overcome the nucleation barrier, so crystallization starts at higher temperatures, whereas at higher χ nuclei become active at lower temperatures [11].

The influence of the filler on dynamic solidification of PET is shown in Fig. 5, which presents the

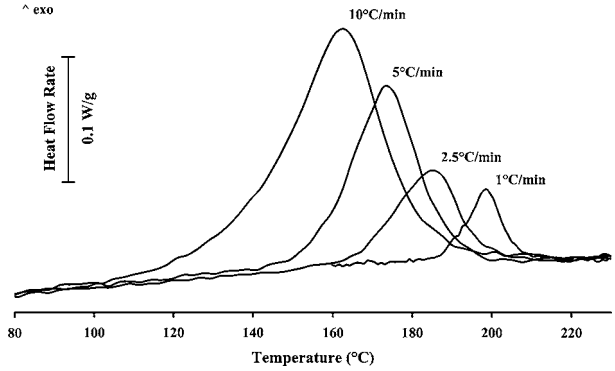

Figure 4 DSC thermoanalytical curves of PET/un-$CaCO_3$ obtained on cooling from the melt at the indicated rates.

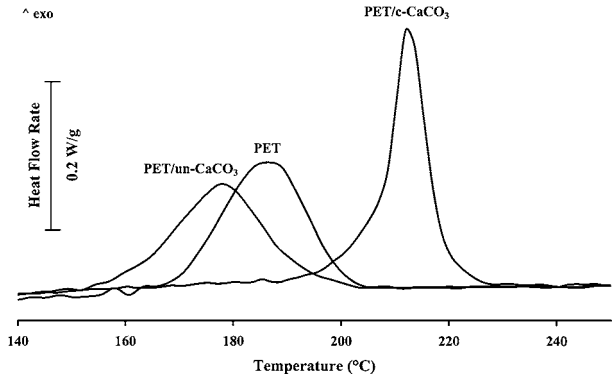

Figure 5 DSC thermoanalytical curves of PET and PET ceramic nanocomposites measured on cooling from the melt at 5°C/min.

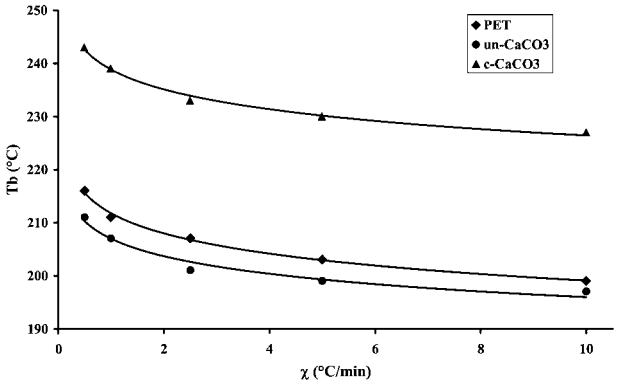

Figure 6 Onset temperature of crystallization (T_b) of PET and PET/$CaCO_3$ nanocomposites as a function of cooling rate.

thermoanalytical curves of PET nanocomposites crystallized at $\chi = 5°C/min$. Similar trends were obtained for the other cooling rates. From the solidification exotherms, the onset temperatures (T_b) were measured and are shown in Fig. 6. In the samples containing added foreign particles, the temperature at which crystallization starts is indicative of the effectiveness of the fillers to promote heterogeneous nucleation [27]. T_b values depend on cooling rate and composition. The addition of $CaCO_3$ coated with stearic acid induces crystallization to start at high temperatures, whereas in the sample containing uncoated $CaCO_3$ solidification from the melt begins at slightly lower temperatures than in plain PET. The presence of stearic acid, promoting good adhesion between the filler and the polyester matrix, facilitates the role of the nanoparticles as effective nucleating agents for PET. Conversely, $CaCO_3$ alone cannot promote nucleation of PET, in agreement with the findings of Xantos *et al.* for carbonate particles of larger dimensions [28], and its presence seems to delay solidification. This is probably a consequence of the increased energy barrier due to the need to reject and/or occlude the ceramic nanoparticles from the solidification front, resulting in a lower crystallization rate [29].

The crystallization exotherms of the PET/c-$CaCO_3$ nanocomposite result much narrower than those of the other two samples, as shown in Fig. 5 for a cooling rate of 5°C/min. For this sample solidification occurs at higher temperatures, where growth rates are lower. The high number of nuclei provided by the nanoparticles induce a large amount of crystallites to grow simultaneously, overweighing the effect of lower growth rates. The large quantity of preformed nuclei in PET/c-$CaCO_3$ produces a steep beginning of the exothermic peak, as shown in Fig. 5, and crystallization is completed in a relatively short time, slowing only when crystallization nears completion, due to termination of growth by impingement. Conversely, in plain PET and in PET/un-$CaCO_3$ nanocomposite a much lower number of effective heterogeneous nuclei, with a relatively broad distribution of induction times, are present, resulting in a more gradual beginning of the solidification exotherm. The overall effect is much a sharper crystallization peak for the PET/c-$CaCO_3$ sample, which supports the hypothesis of effectiveness of c-$CaCO_3$ as nucleating agent for PET.

To analyze the kinetics of the non-isothermal crystallization process, the method proposed by Ozawa [30] was applied. According to Ozawa, the degree of conversion at temperature T is related to the cooling rate χ by the expression:

$$X(T) = 1 - \exp\left[-\frac{K(T)}{\chi^n}\right] \quad (1)$$

where $X(T)$ is the relative crystallinity at temperature T, n is the Avrami exponent, and $K(T)$ is the cooling crystallization function. K is related to the overall crystallization rate and indicates how fast crystallization occurs [31]. Equation 1 can be rewritten as:

$$\text{Log}\{-\ln[1 - X(T)]\} = \text{Log}[K(T)] - n\text{Log}(\chi) \quad (2)$$

By plotting the left term of Equation 2 against Log (χ), a straight line should be obtained and the kinetic parameters n and K can be derived from the slope and the intercept respectively. Previous investigations showed that this method can be applied to analyze the dynamic solidification of plain PET [11].

In Fig. 7 the Log$\{-\ln[1 - X(T)]\}$ vs. Log(χ) plots for the three samples are shown. Experimental data for plain PET and the PET/un-$CaCO_3$ nanocomposite were fitted by straight lines. For plain PET, the Ozawa exponent is about 3, in agreement with literature data [11], and is probably due to heterogeneous nucleation and three-dimensional growth of the crystals. For the PET/un-$CaCO_3$ nanocomposite also $n = 3$ was found,

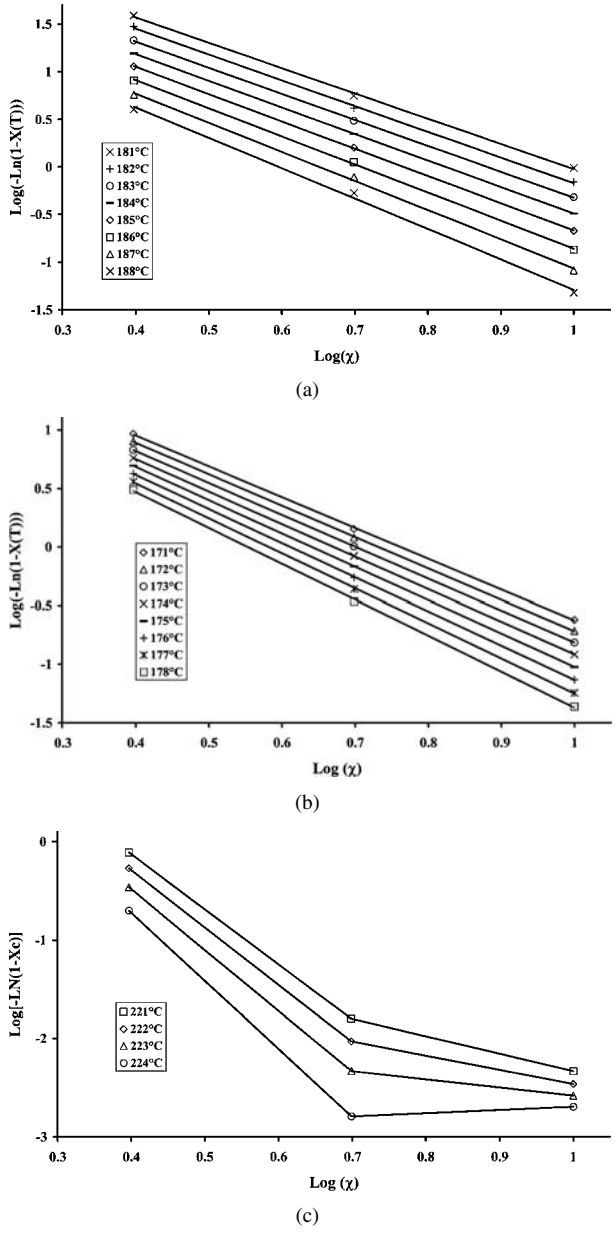

Figure 7 Ozawa plots: (a) plain PET; (b) PET/un-$CaCO_3$; (c) PET/c-$CaCO_3$.

suggesting that the crystallization mechanism of PET is not affected by the presence of this filler. For the PET/c-$CaCO_3$, instead, the Ozawa equation does not provide a satisfactory description of the non-isothermal crystallization kinetics. In order to apply the Ozawa method, the $X(T)$ chosen at a given temperature includes values selected from the earliest stages of crystallization at high cooling rates and values from the end stage at lower rates. At high conversion, crystallization rate is lowered by factors like spherulite impingement and secondary crystallization, and the values may be not comparable with those obtained at early stages of conversion, when nucleation is the rate controlling step. In fact, it has been shown that the Ozawa method cannot describe the non-isothermal solidification process of polymers like polyethylene, poly(ether ether ketone) or nylon 11 where a large portion of the overall crystallization is attributed to slow secondary crystallization [11]. The rapid termination of spherulite growth by impingement due to the high number of growing crystals, coupled with the high crystallization rate at the beginning of the phase transformation, is probably the cause of the non-applicability of the Ozawa method for the PET/c-$CaCO_3$ sample.

The melting behavior of PET and PET/$CaCO_3$ nanocomposites is summarized in the third and fourth columns of Table I, that report the melting temperatures and the crystalline fractions of the three samples, determined from the fusion endotherms of the curves in Fig. 3. In the thermogram relative to plain PET, three melting peaks can be observed. As reported in the literature, the endotherm at low temperature is related to fusion of secondary crystals, the shoulder at about 235°C is due to melting of primary crystals, and the third and main peak is due to melting of the crystals reorganized during the heating scan [32–35]. For both the PET/calcium carbonate samples the endotherm at lower temperatures is still present, whereas the shoulder observable in plain PET merges into the main melting peak.

As reported in Table I, the melting temperature of plain PET is centered at about 251°C and the crystalline percentage of this sample is about 35%. The peak value of the melting endotherm of the sample reinforced with un-$CaCO_3$ (249°C) is only slightly lower, whereas the T_m value of the samples filled with c-$CaCO_3$ is higher (259°C). The crystalline percentage of the sample reinforced with $CaCO_3$ coated with stearic acid is slightly higher than that of plain PET, as shown in Table I, whereas a decrease in the crystalline fraction is observed for the PET/un-$CaCO_3$ sample.

The different crystallinities and melting temperatures of the samples can be attributed to the different effect of the nanoparticles on the crystallization process of PET. Compared to plain PET and PET/un-$CaCO_3$, crystallization of the PET/c-$CaCO_3$ nanocomposite takes place at higher temperatures, where thicker crystals form, which explains the occurrence of fusion at higher temperatures. The lower T_m and crystallinity of the PET/un-$CaCO_3$ sample can be ascribed to the slight hindrance of this filler on the solidification process of the polyester.

4. Conclusions

The *in situ* preparation methodology allows to obtain a good dispersion of the $CaCO_3$ nanoparticles into the poly(ethylene terephthalate) matrix. The coating with stearic acid facilitates the establishment of strong interactions between the nanoparticles and the polyester matrix, resulting in a good adhesion level.

The different compatibility of the two types of nanofillers to the matrix is responsible for the diverse effect of the calcium carbonate nanopowders on the thermal properties of PET. The addition of c-$CaCO_3$ to PET produces a more marked increase in the glass transition temperature and a slightly better thermal stability of the material. Moreover, the calcium carbonate nanoparticles coated with stearic acid are effective nucleating agents for PET. Their presence induces solidification to start at a much higher temperature compared to plain PET and produces a more rapid phase transformation. Conversely, without the inorganic coating, the

$CaCO_3$ nanopowders slightly retard the solidification process of PET.

Acknowledgements

The authors wish to thank Dr. M. Malinconico for his help with the preparation of the nanocomposites and Mr. G. Della Volpe for technical assistance. This work was partially supported by BRITE-EURAM Contract No. CT96-0241, Project No. BE 96-3462.

References

1. E. P. GIANNELLIS, *Adv. Mater.* **8** (1996) 29.
2. J. E. MARK, *Polym. Eng. Sci.* **36** (1996) 2905.
3. T. VON WERNE and T. E. PATTEN, *J. Am. Chem. Soc.* **121** (1999) 7409.
4. P. CALVERT, in "Carbon Nanotubes," edited by T. W. Ebbsen (CRC Press, Boca Raton, FL, 1997) p. 277.
5. V. FAVIER, G. CANOVA, S. C. SHRIVASTAVA and J. Y. CAVAILLE, *Polym. Eng. Sci.* **37** (1997) 1732.
6. L. CHAZEAU, J. Y. CAVALLE, G. CANOVA, R. DEBDIVEL and B. BOUTHERIN, *J. Appl. Polym. Sci.* **71** (1999) 1797.
7. M. ALEXANDRE and P. DUBOIS, *Mat. Sci. Eng.* **28** (2000) 1.
8. Y. OU, F. YANG and Y. ZHUANG, *Acta Polym. Sin.* **2** (1997) 199.
9. M. AVELLA, M. E. ERRICO, S. MARTELLI and E. MARTUSCELLI, *Appl. Organomet. Chem.* **15** (2001) 1.
10. M. AVELLA, M. E. ERRICO and E. MARTUSCELLI, *Nanoletters* **1** (2001) 213.
11. M. L. DI LORENZO and C. SILVESTRE, *Progr. Polym. Sci.* **24** (1999) 917.
12. D. R. LIDE (ed.), "Handbook of Chemistry and Physics," 76th ed. (CRC Press, Boca Raton, FL, 1995).
13. F. B. CRAMER, in "Macromolecular Syntheses," edited by J. A. Moore (John Wiley & Sons, New York, 1977) p. 17.
14. ATHAS Data bank. WWW address on the Internet: http://web.utk.edu/~athas.
15. R. KROKER, S. MANFRED and K. HAMANN, *Progr. Org. Coatings* **1** (1972) 23.
16. W. KLUPP and R. LAIBLE, *Angew. Makromol. Chem.* **57** (1977) 225.
17. N. TSUBOKAWA, K. MURUYAMA, Y. SONE and M. SHIMOMURA, *Polym. Prepr. Jpn.* **37** (1988) 194.
18. *Idem.*, *Polym. J.* **21** (1989) 475.
19. *Idem.*, *Coll. Polym. Sci.* **267** (1989) 511.
20. M. E. BEDNAS, M. DAY, K. HO, R. SANDER and D. M. WILES, *J. Appl. Polym. Sci.* **26** (1981) 277.
21. H. ZIMMERMAN, in "Developments in Polymer Degradation," Vol. 5, edited by N. Grassie (Applied Science, London, 1984) p. 79.
22. M. DZIĘCIOŁ and J. TRESZCZYŃSKI, *J. Appl. Polym. Sci.* **69** (1998) 2377.
23. B. J. BRISCOE, in "Friction and Wear of Polymer Composites," Vol. 1, edited by K. Friedrich, Composite Materials Series, R. B. Pipes series editor (Elsevier, Amsterdam, 1986) p. 31.
24. B. MONASSE and J. M. HAUDIN, *Coll. Polym. Sci.* **117** (1986) 264.
25. M. L. DI LORENZO, S. CIMMINO and C. SILVESTRE, *J. Appl. Polym. Sci.* **82** (2001) 358.
26. M. L. DI LORENZO, *Polymer* **42** (2001) 9441.
27. B. WUNDERLICH, "Macromolecular Physics, Vol. 2, Crystal Nucleation, Growth, Annealing" (Academic Press, New York, 1976).
28. M. XANTOS, B. C. BALTZIS and P. P. HSU, *J. Appl. Polym. Sci.* **64** (1997) 1423.
29. M. L. DI LORENZO, *Progr. Polym. Sci.*, submitted.
30. T. OZAWA, *Polymer* **12** (1971) 150.
31. L. C. LÓPEZ and G. L. WILKENS, *ibid.* **30** (1989) 882.
32. Z. G. WANG, B. S. HSIAO, B. B. SAUER and W. G. KAMPERT, *ibid.* **40** (1999) 4615.
33. G. GROENINCKX, H. REYNAERS, H. BERGMANS and G. SMETS, *J. Polym. Sci. Phys.* **29** (1980) 7491.
34. Y. LEE and R. S. PORTER, *Macromolecules* **20** (1987) 1336.
35. P. J. HOLDSWORTH and A. TURNER-JONES, *Polymer* **12** (1971) 195.

Received 14 March 2001
and accepted 7 February 2002